Microbiome-inspired phyllospheric synthetic communities increase microbial diversity and productivity of field-grown plants of Agave tequilana

Víctor Flores-Núñez
Centro de Investigación y de Estudios Avanzados del IPN (Cinvestav) - Irapuato
David Camarena-Pozos
Centro de Investigación y de Estudios Avanzados del IPN (Cinvestav) - Irapuato
Daniel Chávez-González
Centro de Investigación y de Estudios Avanzados del IPN (Cinvestav) - Irapuato
Raúl Alcalde-Vázquez
Centro de Investigación y de Estudios Avanzados del IPN (Cinvestav) - Irapuato
Nélida Vázquez-Sánchez
Centro de Investigación y de Estudios Avanzados del IPN (Cinvestav) - Irapuato
Alan Hernández-Melgar
Centro de Investigación Científica y de Educación Superior de Ensenada
Jorge Xool-Tamayo
Centro de Investigación Científica y de Educación Superior de Ensenada
Aldo Moreno-Ulloa
Centro de Investigación Científica y de Educación Superior de Ensenada
Laila Partida-Martínez (laila.partida@cinvestav.mx)
Centro de Investigación y de Estudios Avanzados del IPN (Cinvestav) - Irapuato https://orcid.org/0000-0001-8037-2856

Article

Keywords:

Posted Date: July 1st, 2022

DOI: https://doi.org/10.21203/rs.3.rs-1782141/v1

TITLE

Microbiome-inspired phyllospheric synthetic communities increase microbial diversity and productivity of field-grown plants of *Agave tequilana*

Víctor M. Flores-Núñez[1,a], David A. Camarena-Pozos[1,b], J. Daniel Chávez-González[1], Raúl Alcalde-Vázquez[1], M. Nélida Vázquez-Sánchez[1], Alan G. Hernández-Melgar[2], Jorge Xool-Tamayo[2], Aldo Moreno-Ulloa[2] and Laila P. Partida Martínez[1*]

[1] Departamento de Ingeniería Genética, Centro de Investigación y de Estudios Avanzados del Instituto Politécnico Nacional (Cinvestav), Irapuato 36824, México

[2] Departamento de Innovación Biomédica, Centro de Investigación Científica y de Educación Superior de Ensenada, Baja California (CICESE), Ensenada 22860, México

[a] Present address: Christian-Albrechts University of Kiel, Kiel 24118, Germany

[b] Present address: Centro de Innovación Aplicada en Tecnologías Competitivas (CIATEC), León 37545, México

***Corresponding author:** Laila P. Partida-Martínez (laila.partida@cinvestav.mx).

Km. 9.6 Lib. Nte. Carr. Irapuato-León. 36824 Irapuato, Gto., México.

ABSTRACT

Agaves are plants native to North America that sustain life in arid and semi-arid ecosystems.

Previous studies revealed that cultivated plants of *Agave tequilana* had lower microbial diversity and functionality compared to wild species. Here, we tested if microbiome-inspired phyllospheric synthetic communities, based on microbial hubs or enriched phyllospheric microbial functions, could increase microbial diversity and plant fitness in *A. tequilana*.

We applied seven functional and three random syncoms on one-year-old plants of *A. tequilana* in the field and monitored their development for two years. Phylogenetic analyses revealed that the composition and diversity of the phyllospheric prokaryotic and eukaryotic communities associated with *A. tequilana* were affected by the season, with greatest diversity observed during the dry months. The addition of functional syncoms promoted phyllospheric microbial communities with a higher diversity, greater capacity to consume carbon sources, and more integrated and complex networks. Additionally, plants treated with functional syncoms had an increased content of sugars (^{o}Brix, a measure of productivity in agaves) in the stems, and higher leaf metabolic diversity.

Our work demonstrates that inoculation of syncoms formulated based on functional analyses of microbiome data represents an effective biotechnological tool to improve the sustainability and productivity of crops of arid ecosystems.

INTRODUCTION

Plants of the genus *Agave* originated in the arid and semi-arid regions of North America, reaching their peak of diversity and endemism in Mexico[1]. Agaves have been used by humans since pre-hispanic times, and are intensively cultivated to produce alcoholic distilled beverages, such as Tequila produced from plants of *Agave tequilana* Weber var. Azul[2].

In 2020, production of Tequila for the local and international markets required the fermentation of 1.3 million tons of five-to-seven-years-old mature *A. tequilana* stems, and annual sales of Tequila reached on average of 51.2 billion MXP in 2019-21 (https://www.crt.org.mx, https://www.statista.com). Plant productivity, and the consequent selling price of *A. tequilana*, depends heavily on the amount of sugars (measured as °Brix) and biomass in the stems. As the Tequila market continues expanding (https://acevesspirits.com/), producers of *Agave* plants require sustainable methods to foster plant productivity and health.

Our research on the *Agave* microbiome has revealed that microbial communities associated with wild and cultivated plants of this genus are diverse and structured, and that their composition and diversity is dependent on the plant compartment and the biogeography of the host plants[3]. Also, it has shown that the associated microbiome and their emitted volatile organic compounds can effectively promote growth and development of agaves and other plants[4,5].

Remarkably, we identified that cultivated *A. tequilana* showed reduced microbial diversity in the rhizosphere and phyllosphere compared to wild *A. deserti* and *A. salmiana*[3]. This lower diversity was also observed when analyzing microbial functions using shotgun metagenomics. Particularly, the phyllosphere of *A. tequilana* plants had a reduced number of genes related to phototrophy, carbon metabolism, secondary metabolites biosynthesis and xenobiotic degradation[6]. However, it was unclear if the addition of potentially keystone microorganisms could enhance microbial diversity, and if such an increase could improve plant fitness in this agriculturally managed *Agave* species.

In the present study, we designed seven functional synthetic communities (syncoms) inspired by two concepts: 1) keystone taxa resulting from network analyses (also called microbial hubs[7], V. M. F.-N, Citlali Fonseca-García, Damaris Desgarennes and L. P. P.-M. *in press,* Fig S1a); and 2) taxa with enrichment in specified functional traits in the phyllosphere (e.g. phototrophy[6], Fig S1b). These syncoms were inoculated in one-year-old plants of *Agave tequilana* in the field (Fig. S2, Table S1), and their impact on microbiome composition

and plant fitness were compared against three random syncoms (Fig S1c), and non-inoculated plants (MOCK).

We employed amplicon sequencing of the 16S rRNA and ITS2 genes, Biolog profiling, and plant developmental and physiological measurements (height, diameter, number of leaves, number of rhizomatic suckers, sugars concentration in the stem and plant metabolomics) to determine microbial composition, alpha and beta diversity, network complexity in the phyllosphere, as well as plant fitness across a span of two years (Fig. S3).

Our work shows that the microbial communities associated with the phyllosphere of *A. tequilana* respond to the season, being more diverse in the dry months. We demonstrate that a subset of functional syncoms promoted microbial diversity and functionality, as well as the complexity and integration of the phyllospheric microbial networks. These syncoms also positively impacted plant productivity (°Brix) and significantly changed the leaf metabolome of their host plants. In sum, our work shows how microbiome-based knowledge can be successfully used to improve the effectiveness of biofertilizers in crops of drylands.

RESULTS

The phyllosphere of field-grown *A. tequilana.*

We analyzed the prokaryotic and eukaryotic communities associated with the phyllosphere of *A. tequilana* after the inoculation of syncoms inspired in the microbiome of *Agave* species. Syncoms were designed based on highly connected and central OTUs in correlation networks (PFC, PFCF, PFCS, and PFCT), enriched microbial functions in the phyllosphere (AAP, CC, BC) or by selecting strains randomly (RC1, RC2, RC3). The microbial suspensions were sprayed on the leaf surface of one-year-old, field-grown *A. tequilana* plants in November 2019 (t0), and the microbial communities were evaluated at 3-, 8-, and 12-months post inoculation (t3, t8 and t12, respectively, Fig. S3).

Across all samples, 19 prokaryotic phyla were detected. Proteobacteria, Actinobacteria, Bacteroidetes, and Firmicutes comprised on average 94.7% of the relative abundance (Fig. S4a). Burkholderiales, Micrococcales, Cytophagales, and Bacillales were the most abundant orders in each phylum, respectively (Fig. 1a). Seven eukaryotic phyla were detected. Ascomycota and Basidiomycota comprised on average 87.9% of the relative abundance (Fig. S4b). Pleosporales and Tremellales were the most abundant orders in each phylum, respectively (Fig. 1b).

The order Caulobacterales was enriched in the rainy period (t8, Fig. 1a, Table S2) together with 26 OTUs, most of them classified as Proteobacteria (16, 61.5%) and Bacteroidetes (5, 19.2%) (Table S3). During the dry period (t3 and t12), Kineosporiales and other low abundance orders were enriched (Table S2). Also, 222 OTUs including Actinobacteria (46, 20.7%), Bacteroidetes (28, 12.6%), Firmicutes (18, 8.1%) and Proteobacteria (Burkholderiales 10%, Rhizobiales 12.6%, Sphingomonadales, 10%, Table S3).

Agaricales, Melanosporales and Filobasidiales were fungal orders enriched in the rainy period, while Chaetothyriales, Cystobasidiomycetes, Erysiphales and Trichosphaeriales were more abundant in the dry period (Fig. 1b, Table S2). Several OTUs were enriched in both seasons (238 dry, 138 rainy) belonging to diverse orders, but primarily Pleosporales or unclassified (Table S4).

PERMANOVA analyses of the binary Bray-Curtis distances between samples showed that the sampling season had the most influence on the microbial communities (Table S5). This factor explained 14.2% and 27.4% of the variance in the prokaryotic and eukaryotic communities, respectively. The sampling block and treatment had a significant but smaller influence on these communities. We observed that few OTUs were enriched in the syncom-

derived communities (Fig. S5). NMDS ordination analyses showed that most samples tend to cluster together in the prokaryotic communities, but the rainy season samples were the most dissimilar (Fig. 2a). In the eukaryotic communities, samples cluster more clearly based on the sampling season (Fig. 2b).

In the rainy season, there was a significant reduction in alpha diversity and an increase in the variability of the prokaryotic and eukaryotic microbial communities (Fig. 2). The position in the field did affect the diversity of the eukaryotic communities (Fig. S6), probably as a result of the different presence of weeds. We observed more weeds in block A than in B (Fig. S2a).

Temporal variation of syncoms.

The sequenced 16S-rRNA-V4 or ITS2 region of the 31 inoculated strains matched with at least one OTU (97% and 95% of similarity, respectively, Table S6). Based on the syncom composition, treatments were grouped in Network (PFC, PFCF, PFCS, PFCT), Metagenome (AAP, CC, BC), and Random (RC1, RC2, RC3) to evaluate the enrichment of the inoculated strains at t0. *Belnapia rosea* MJ22, *Methylobacterium* sp RAS18, and *Micrococcus aloeverae* RAT4 were more abundant in plants inoculated with Network syncoms than in the rest of the plants. These OTUs maintained a low abundance after inoculation (0.57, 0.12, and 0.02% of mean relative abundance, respectively, Fig. S7).

B. rosea MJ22, *Kineococcus radiotolerans* AS2.23, *Methylobacterium* sp. RAS18, *M. aloverae* RAT4, *Rhizobium* sp. RAS22, *Sphingomonas aerolata* AS2.4, and *Sphingomonas endophytica* AS3.13 were more abundant at t0 than at t3 only in plants inoculated with Network and Metagenome syncoms. Several strains had reduced abundance at t8 (rainy period) and increased again at t12 (Fig. S7).

Syncoms increased the alpha diversity and microbial interactions in the phyllosphere.

A subset of syncoms inoculated on the leaves of *A. tequilana* were observed to affect the diversity of their phyllospheric prokaryotic communities. The phyllosphere promoted by PFCS had a higher prokaryotic alpha diversity than control plants (MOCK, Fig. 3a, Fig. S8a). This effect was maintained until t8, when this phyllosphere showed the greatest increase in OTU richness and Shannon index (0.89 and 0.66 log2 fold change (FC) compared to MOCK, Fig. 3a, Fig. S8a). Syncoms PFC and BC also increased OTU richness in February (Fig. S8a). These syncoms did not influenced the diversity of eukaryotic communities. Only RC2 increased the OTU richness (Fig. S8b), while CC increased alpha diversity at t3 compared to the control (Fig. 3b, Fig. S8b).

Community metabolic profiling was assessed in the second rainy season (June 2021, t19, Fig. 3c) as a proxy for microbial diversity and functionality. The phyllospheric communities of plants inoculated with PFC, PFCF, PFCS, and RC2 consumed a more diverse array of carbon sources than the MOCK-derived microbial communities. Most of these compounds corresponded to simple sugars and organic acids.

Correlation networks in the treated plants had more OTUs and correlations than non-inoculated controls (Fig. 4, Fig. S9a). Moreover, most syncoms increased prokaryotic-eukaryotic correlations and decreased the eukaryotic-eukaryotic ones (Fig. 4, Fig. S9b). The phyllosphere derived from PFCS had more than two times the number of hub OTUs compared to MOCK plants and the rest of the syncoms (Fig. 4, Table S7). Moreover, the genera present in syncoms were present as microbial hubs. OTU 43 (*Methylobacterium*) was a hub in non-inoculated and inoculated plants. OTUs classified as *Sphingomonas* (OTU 18, 89, 164, and 167*)*, *Methylobacterium* (OTU 113), and *Nocardioides* (OTU 271) were microbial hubs in PFCS-inoculated plants. Finally, *Bacillus* (OTU 14) and *Massilia* (OTU 481) were microbial hubs in plants inoculated with PFCT (Fig. 4, Table S7).

Syncoms influenced the growth and physiology of field-grown *A. tequilana.*

The growth rate of plants increased in the first year after inoculation with syncoms (Fig. 5a), and no signs or symptoms of plant disease were recorded. The changes in height were greater in plants inoculated with PFCT and RC3 (0.86 and 0.54 FC, respectively, compared to MOCK with 1.54 cm/month) while plants inoculated with PFC and RC1 syncoms unfolded more leaves (0.4 and 0.33 FC, respectively, compared to MOCK with 2.14 leaves/month. Only the plants inoculated with the CC syncom grew at a higher rate than the control during the second year.

The plants inoculated with the AAP syncom diminished their growth. The growth rate of these plants was lower in both years (-0.86 and -0.51 FC in height compared to MOCK, Fig. 5a) and produced fewer rhizomatic suckers after 1 year (-0.64 FC, compared to MOCK with 2.8 rhizomatic suckers, Fig. 5b).

The concentration of sugars in the stem sap did not change significantly until two years after the inoculation with syncoms (t24). Plants inoculated with PFC, PFCS and AAP increased the concentration of the °brix in the stem sap by 0.64, 0.38, and 0.42 FC, respectively, compared to the control with 13.16 ºBrix (Fig. 5c).

PFCS and PFCT syncoms influenced the plant metabolome of field-grown *A. tequilana.*

Untargeted metabolomics in the leaves of field-grown *A. tequilana* plants inoculated with PFCS, PFCT, and MOCK was performed in t12. LC-MS^2 data extraction by MZmine and filtering by Metaboanalyst retrieved 1,520 potential metabolites with reproducible quantification. As shown in Fig. 6a, the first and second principal components separated PFCS- and PFCT-treated plants on both sides of the graph, hinting at distinct biological effects. Heatmap representation and hierarchical clustering analysis showed specific patterns between datasets using the top-50 most significant features (Fig. 6b). The volcano plots revealed differential effects by PFCS and PFCT on the *Agave* metabolome based on the number of modulated metabolites (Fig. 6c,d). Globally, more metabolites were modulated by PFCS (n=184) compared to PFCT (n=56), and of those, a low overlap among syncom treatments (at the MS1 level) was inferred by UpSet plot analysis (Fig. 6e). As shown in Fig. 6f, a higher repertoire of chemical classes assigned to the up- (36% annotation rate) and down-modulated (30% annotation rate) metabolites were noted in the PFCS-treated *Agave* plants compared to the PFCT group (Fig. 6e). The chemical classes "organooxygen compounds" and "carboxylic acids and derivatives" were predominantly down-modulated and up-modulated by PFCS treatment, respectively. The complete list of putative annotated metabolites (MSI, level 3) aided by CANOPUS and CSI: FingerID tools are described in Table S12 and Table S13. Due to the challenging task of characterizing the entire metabolites (at the molecular structure) modulated by treatments, we further guided our analysis based on molecular networking and spectral matching annotation (MSI, level 2) by the GNPS online platform as previously shown[8]. Our strategy enabled us to confidently annotate (aided by CSI: FingerID and MolDiscovery tools) a group of carbohydrate derivatives belonging to the class of the "organooxygen compounds" that was down-regulated by PFCS treatment, but not by the PFCT (Fig. S10). Further work should reveal in which specific plant metabolic processes these compounds are involved in agaves

DISCUSSION

Our work shows that phyllospheric microbial communities associated with *A. tequilana* were affected by seasonal variations and remarkably displayed higher diversity during the dry months. This pattern contrasts with the decreases in bacterial and fungal diversity observed in the rhizosphere of *Opuntia ficus-indica* along an aridity gradient[9,10], suggesting that below- and above-ground epiphytic microbial communities respond differently to aridity. Other study in the Mediterranean semi-arid ecosystem found, similarly to our research, that fungal communities associated with eight sympatric and perennial plants differentiated based on the season, being more similar in the hot and dry summers than in the mild and wet winters[11].

Importantly, our work demonstrates that phyllospheric microbial communities associated with *A. tequilana* can be manipulated with the inoculation of microbiome-inspired syncoms. The syncoms based on networks (PFC, PFCF, PFCS, and PFCT) were formulated with taxa presenting high centrality and connectivity in correlation networks of the phyllosphere of wild *A. salmiana* and cultivated *A. tequilana* (Table S1, V. M. F.-N, Citlali Fonseca-García, Damaris Desgarennes and L. P. P.-M. *in press*). Therefore, we expected them to act as keystone microorganisms that will have a major influence on the assembly of microbial communities[7,12,13]. *B. rosea* MJ22 and *Methylobacterium* sp. RAS18 are aerobic anoxygenic phototrophs bacteria[6] present in all network syncoms, but they alone can not explain the changes in diversity. The addition of other common keystone bacteria (as in PFC) resulted in a higher prokaryotic diversity at t3, highlighting the complementarity of diverse taxa, such as Actinobacteria and Firmicutes, as a force driving this effect. Moreover, the addition of *A. salmiana* strains (PFCS, *Sphingomonas* spp., *Frigoribacterium endophyticum* AS3.20, *Cellulomonas cellase*a RAS26, and fungi) was relevant for maintaining a high prokaryotic diversity at t8, when it reached the lowest values. The additive effect was absent when adding fungal strains alone (PFCF) or *A. tequilana*'s hubs (PFCT). This evidences is in agreement with the increase in microbial diversity shown in other plants after the inoculation of biofertilizers[14,15], but contrasting results have been reported[16]. Together, this evidence supports that microbial hub's influence on community structure depends on the arising microbe-microbe interactions and the environment[7,17].

The inoculation of syncoms resulted in more complex and integrated correlation networks. This phenomenon was also found in the bulk soil of wheat[18], the phyllosphere of tobacco[19], and the rhizosphere of tea[15] plants after inoculation with native and non-native bacterial consortia, suggesting that the addition of native or non-native microorganisms can modify

the way that phyllospheric microorganisms interact, even in plants with established microbiomes. Remarkably, only the phyllosphere derived from PFCS had a greater amount of hub OTUs, some of them from the same taxa as the inoculated bacteria (*Sphingomonas, Methylobacterium, Nocardioides*). *Sphingomonas* spp. were the main component of PFCS, and *S. endophytica* AS3.13, *Methylobacterium* sp. RAS18, and *F. endophyticum* AS3.20 correlated with the hub OTUs in the PFCS network (Fig S11), suggesting that the inoculated bacteria could be reinforcing native microbiota to act as hubs similar to the keystone reinforcement concept[12]. This result also highlights the relevance of *Sphingomonas* species in the plant phyllosphere, a genus that has also been found as keystone taxa in *A. thaliana*[20]*.* In contrast, the phyllosphere derived from PFCT had the same inoculated *M. aurea* as microbial hub, suggesting its adaptation to the cultivated plants of *A. tequilana*.

Importantly, our work corroborates the hypothesis that the augmentation of hubs from wild *A. salmiana* (PFCS) in the cultivated species *A. tequilana*, that has lower microbial diversity, contributes to a more diverse microbiome and a more integrated correlation network with relevant microbial hubs that resemble the microbiome of wild *Agave* species (V. M. F.-N, Citlali Fonseca-García, Damaris Desgarennes and L. P. P.-M. *in press)*. These wild-like microbial communities could be more resistant to pathogen invasion and other environmental stresses and perturbations[12,21,22].

Other syncoms also showed increments in alpha diversity. BC syncom was formed with taxa that represented most of the enriched biofilm and quorum sensing (QS) genes in the phyllosphere[6]. Biofilm formation has been associated with changes in the plant microbiome[23] and the ability of immigrant bacteria to colonize the leaves[24]. Moreover, the genomic annotation of Network and Random syncom members have shown that they possess genes related to biofilm formation and QS (Fig S12), which warrants more research to assess their influence on community structure. Even RC2 increased the OTU richness of the eukaryotic phyllosphere, highlighting the possibility of functional redundancy or other microbial processes that were not targeted in our experimental design.

The selection of strains for bio-inoculants has been mainly based on the presence, frequency and intensity of canonical plant growth promotion traits (e. g. the selection of biofertilizers for arid lands[25]) but without knowledge of their influence on the native microbial community or their persistence. Our work sets the precedent for the selection of functional strains based on their putative interactions within the microbial communities, and their ability to influence plant growth in agroecosystems. Both approaches can coexist now that multiple microbial genomes and amplicon sequencing data sets for several plant species are available. Here, we show that syncoms inspired in the *Agave* microbiome represent valuable

alternatives for agriculture, as they can persist in the plant tissues in the context of the environment and the indigenous microbiota[26]. Additionally, the phyllosphere derived from PFC, PFCF, PFCS and RC2 were metabolically more diverse in the second rainy season (t19), suggesting a long-term effect of the inoculated syncoms under natural field conditions.

Microbiome research have postulated different hypothesis about the relationship between microbial diversity and plant fitness[13]. We did not find a significant correlation between plant growth and microbial diversity nor OTU absolute abundance (not shown). Instead, both functional (PFC, PFCT) and random communities (RC1, RC3) increase at least one growth parameter during the first year, suggesting that diverse microorganisms can influence plant growth independently from their network position or known functions. The unfolding of leaves in agaves correlates with the environmental productivity index[27], a parameter that was increased by both PFC and RC1 syncoms. Moreover, stem sugars are the primary raw material for Tequila production. Syncoms PFC, PFCS, and AAP increased the number of sugars in the stem after 2 years post-inoculation which is indicative of a higher yield. Contrary to most of the works demonstrating the plant growth promoting effect of *Methylobacterium*[28,29], in *A. tequilana* AAP bacteria alone reduced the growth of the plants, but the rest of the PFC bacteria supported their growth, highlighting the relevance of using more diverse microbial inoculants. Inoculated strains could have influenced plant development and growth directly via plant growth promotion traits, including VOCs[4]. Whether inoculated bacteria and fungi influenced growth directly or indirectly via attracting functional microorganisms[12] remains to be tested.

The inoculated syncoms (PFCS, PFCT), formulated with common and specific keystone taxa (*A. salmiana* and *A. tequilana*, respectively), interacted with the plants causing a differential production of leaf metabolites after 12 months of the inoculation. PFCS-inoculation modulated several benzene and steroidal compounds (e. g. saponins). These group of metabolites are common in plants of the genus *Agave* [30,31], and the phyllospheric microbiome of wild A. *salmiana* and cacti harbors abundant and diverse genes related to the degradation of these compounds (V. M. F.-N, Citlali Fonseca-García, Damaris Desgarennes and L. P. P.-M. *in press)*. The biggest group of down-regulated metabolites in PFCS plants were organooxygen compounds that include many carbohydrate derivatives. Despite not being able to link them to the biosynthesis of fructans, this decrease inversely correlated with the changes in sugar accumulation in the stem. Moreover, a steroidal saponin, commonly named as yuccalan, was found down-regulated in PFCS plants. This compound was discovered on the leaves of *Yucca* and has antifungal activity[32]. These results support the notion that syncoms not only influence microbe-microbe interactions, but also the metabolic

interactions of the host plant and the microbial community with long lasting effects. Further work is needed to understand the plant metabolic processes that are more prone to be affected by the associated microbiota, and their consequences for plant health and productivity.

Altogether, our work offers direct evidence that the selection of microbial inoculants inspired by microbiome knowledge is a promising avenue for improving and sustaining plant health and productivity in keystone desert crop species, such as *Agave tequilana.*

ONLINE METHODS

Design of the field experiment

The field experiment was performed in collaboration with Tequila Real de Pénjamo S.A. de C.V. For this, rhizomatic suckers of *Agave tequilana* Weber var. Azul were planted in July 2018 in a 1-ha lot located in Pénjamo, Guanajuato, Mexico (Lat. 20.387444, Long. -101.76425, Altitude 1768 m) (Fig. S2a,b). The distance between plants was ca. 1 m within rows and ca. 3 m between rows. The rhizomatic suckers were treated with a pre-emergent herbicide (Diuron) and a foliar pesticide (Malathion) before planting. Watering was completely dependent on the seasonal rains and no agrochemicals were applied for two years, until July 2020 when the managers applied an insecticide to prevent the development of *Scyphophorus acupunctatus* larvae (picudo).

The field was divided into two blocks east (A) and west (B). Each block was divided into squares of 4 x 20 plants = 80 plants. Block A and B harbored 1000 and 1200 plants approximately and were divided into 12 and 15 squares, respectively. The 10 syncom treatments plus the non-inoculated control were randomized in each block using semi-random numbers.

Bulk soil samples were taken at the beginning of the experiment and after 12 months, both at five representative points for each block. Samples were taken 10–15 cm from the surface using a shovel and stored in clean plastic containers at 4°C. Soil physicochemical characteristics were determined by the company Fertilab (Celaya, Gto., Mexico).

Isolation of phyllospheric microorganisms

Agave leaf samples were processed as previously described[33] with some modifications. Two leaves per individual of three *A. tequilana* F.A.C. Weber and *A. salmiana* Otto ex Salm subsp*. crassispina* (Trel.) Gentry plants were collected in September 2017. *Agave tequilana* leaves were sampled from a cultivated population in Pénjamo, Guanajuato, Mexico, (Lat. 20.686, Long. - 101.875, Altitude 1714 m, Tequila Real de Pénjamo) while *A. salmiana* leaves were sampled from a wild population in San Felipe, Guanajuato, Mexico (Lat. 21.766, Long. -100.163, Altitude 2089 m)). Leaves were obtained using gloves with a sanitized knife. Samples were transported in new brown paper envelopes and maintained in refrigeration until processing. In a laminar flow hood, the leaves were washed with sterile distilled water, then the leaf surface was brushed constantly with a sterile toothbrush and 50 ml of removal buffer (6.75 g KH_2PO_4, 8.75 g K_2HPO_4, and 20 µL of Triton X-100 per liter) inside of a 2 L

plastic sterile beaker. The resulting suspension was transferred to a conic tube. The pellet was obtained by centrifugation at 5000 rpm at 18°C for 15 min and resuspended in 5 ml of removal buffer.

Phyllosphere suspensions were ten-fold diluted in saline solution (NaCl 0.85%). A 100 µL aliquote of each dilution was plated onto TSA (Difco™), Czapek-Dox (Merk™ formulation) , ISP3 (HIMEDIA formulation), ISP5 (HIMEDIA formulation) for heterotrophic bacteria, and PDA (Difco™) for fungi. Plates were incubated for 1-3 weeks at 28°C. Bacterial-like colonies with different morphologies were sub-cultivated on TSA, while filamentous fungi and yeast-like colonies with different morphologies were sub-cultivated on PDA. Only microorganisms with a unique colony and microscopic morphology were selected for further analyses.

Axenic and monoclonal cultures of bacteria and yeasts were obtained by dilution and plating on TSA plates, while axenic cultures of filamentous fungi by subculturing small mycelial plugs in PDA plates. Strains were stored in glycerol 40% at -80°C and -20°C for long and medium-term storage, respectively

Bacterial and fungal strains were identified by amplifying and sequencing the 16S-rRNA gene and the ITS, respectively, as previously reported[33] (Table S8).

Selection of synthetic communities (Syncoms)

Synthetic communities were designed based on previous analyses of the *Agave* and cacti microbiome (Table S1). Highly connected and central taxa (microbial hubs) were identified in correlation networks of amplicon sequence data (V. M. F.-N, Citlali Fonseca-García, Damaris Desgarennes and L. P. P.-M. *in press)* and phyllosphere enriched functions were identified using comparative metagenomics[6]. Microorganisms were selected from the culture collection based on their 16S-rRNA or ITS2 sequence identity to the species level (97% and 95%, respectively) or their genera when no exact matches were found.

Predicted functional communities (PFC) were composed of taxa that were consistently highly connected and central in both wild *A. salmiana* and cultivated *A. tequilana* correlation networks. Other microorganisms were incorporated to test the additional influence of fungal hubs (PFCF), *A. salmiana* specific hubs (PFCS), and *A. tequilana* specific hubs (PFCT). A group of aerobic anoxygenic phototrophs (AAP), cyanobacteria (CC), and known biofilm-producing Proteobacteria (BC) were selected to represent the phyllosphere enriched functions. Randomly selected syncoms were designed by selecting strains from the collection using semi-random numbers (RC1 and RC2) or by a personal selection of strains (RC3) (Table S1).

The partial 16S-rRNA sequences of the selected bacteria were submitted under the accession numbers ON217552-ON217580. The partial ITS sequences of the selected fungi were submitted under the accession number MT488313 and MT488312 (Table S8).

Cultivation of bacterial and fungal strains for syncoms inoculation

Bacteria and yeast strains were recovered from storage in TSA plates after 1-5 days at 28°C. Pre-inocula were prepared by inoculating one colony in 20 ml or 50 ml of liquid media (TSB Difco™), for rapid and slow-growing strains, respectively. Liquid cultures were incubated from 1 to 5 days at 28°C with constant shaking (ca. 120 rpm). The pre-inocula were inoculated (1% v/v) in the appropriate amount of fresh liquid media and incubated from 1 to 3 days at 28°C with agitation (120rpm). All the cultures were taken out from incubation in the exponential phase at the same time and the OD was determined at 600 nm using a Spectrophotometer (Table S9). The purity and axenity of pre-inocula and inocula were assessed visually with the color of the pellet after centrifugation (10000 rpm 2 min), by sub-cultivation in TSA, and by gram staining.

Cladosporium. sp. cutV was recovered from storage in PDA plates after 7–14 days at 28°C. It was inoculated in fresh PDA plates using a sterile toothpick and incubated for three weeks at 28°C until the development of conidia. Conidia were harvested with 5 ml of Triton-100X 0.1% per plate, the suspensions of conidia were then filtered through a sterile polyester mesh to remove big chunks of mycelia and finally counted in a Neubauer chamber. Pre-inoculum and inoculum axenity were determined by macroscopic and microscopic morphology.

We were unable to accurately quantify the number of colony-forming units of cyanobacterial strains because they are filamentous and formed biofilms in liquid and solid media. Filaments of 3-week-old *Leptolyngbya* sp. AT32P and *Nodosilinea* sp. AT21F cultures were inoculated in 1L of fresh Gromov-21 media each and incubated for 3 weeks in a photoperiod room of 16/8h at 28°C. The purity of the pre-inocula and inocula was determined by macroscopic and microscopic morphology.

Inoculation of plants on the field

Syncoms were formulated the day before inoculation. The amount of bacterial culture necessary to prepare 2.5 L (500 ml x 5 plants) of syncoms suspensions with $1x10^6$ CFU/ml of each strain was calculated based on the OD of each liquid culture and conidia suspension. These aliquots were mixed to obtain two concentrated suspensions of each syncom (50 ml, $1.25x10^9$ CFU/ml per strain). Concentrated syncoms were centrifuged

(10000 rpm, 10 min) to remove remaining culture media, resuspended in NaCl 0.85%, and kept at 4°C.

The presence of the strains was validated with a viable count of the mixtures (Table S10). Bacterial and fungal colonies were counted based on their morphological features. Cyanobacteria formed a biofilm in the plates, and we were unable to count them appropriately.

Plants were inoculated in November 2019. On the day of the inoculation, syncoms suspensions were kept on ice until needed. Each suspension was diluted in 1.2 L of tap water in clean plastic bottles and mixed to break any clumps. Each plant was sprayed with 50 ml of the diluted syncoms suspensions ($1x10^6$ CFU/ml each strain) using a hand sprayer. Approximately, 24 plants were sprayed per treatment (8 plants per row) in each block. Non-inoculated or control plants were sprayed with tap water (MOCK). The first two plants in each row and one row between squares were not treated in any way to create a biological barrier between treatments (Fig. S2c).

Plant measurements and sampling

The number of leaves, as well as the diameter and height of the *A. tequilana* plants was measured in November 2019 (dry season, fall, t0, beginning of the experiment), February 2020 (dry season, winter, t3), July 2020 (rainy season, summer, t8), November 2020 (t12), and finally in June 2020 (rainy season, summer, t19). Plant measurements were taken from the same six plants per treatment to determine the growth rate in each treatment during the first year. From November 2019 to June 2021 only the height and width of 30 plants per treatment were recorded. The number of rhizomatic suckers was recorded at 12 and 24 months post-inoculation (Figure S3).

The sugar content of the stem sap was estimated *in situ* in November 2020, June, and November 2021 (t12, t19, and t24, respectively, Figure S3). The stem was drilled with an 8 mm drill, the extracted tissue was pressed in a small garlic press and the sap was collected on a refractometer. Six plants per square were measured.

Two leaves per individual plant were sampled to recover the phyllospheric microbial communities. At the t0, one individual per treatment in each block was sampled, while three individuals per treatment in each block were sampled at t3, t8, t12, and t19. In total 232 individuals were sampled. Leaves from the second and third row of the *Agave* rosette were sampled as explained above.

Assessment of phyllospheric communities

Sample processing

The phyllospheric microorganisms were recovered by brushing the leaf surface with a toothbrush soaked in the washing buffer as explained above. The microbial pellet was covered in 5 ml of absolute ethanol and stored at -80°C until the DNA extraction. The metagenomic DNA was extracted using the DNAeasy Power soil kit (Qiagen) from t0, t3, t8 and t12 sampling points. DNA was recovered in 75 µl of TRIS elution buffer. The quantity and quality of gDNA were recorded using a nanodrop and the recovered DNA was stored at -20°C.

The 240 samples were randomized in 96 well microplates in ranges of 50 to 600 ng of DNA. The samples were sent to *AIM – Advanced Identification Methods* in Leipzig, Germany where the metabarcoding sequencing was performed. The 515F/816R and ITS9F/ITS4R primers were used for the amplification of the 16S-rRNA-V4 and ITS2 regions, respectively. Peptide nucleic acid (PNAs) were added in the 16S-rRNA-V4 reactions to reduce the amplification of plant chloroplast and mitochondrial DNA[34]. After ligation, the paired-end 2x300 bp sequencing was performed in an Illumina MiSeq v3 instrument.

Data was demultiplexed resulting in 240 libraries for the 16S-rRNA-V4 and ITS2, each. Overall data quality was analyzed using FastQC[35] under the Nephele server[36]. An in-house command-line pipeline was designed to process the raw reads (github.com/vicflonun/AgaviSyncoms, Table S11). First, low-quality bases and reads were trimmed using Trimmomatic[37] and the resulting read pairs were assembled using FLASH[38]. The VSEARCH[39] pipeline was used to process the resulting 21,735,602 and 12,391,310 merged pairs for 16S-rRNA-V4 and ITS2, respectively. Before clustering, all the merged pairs were renamed, the primers and remaining adapters were cropped from the 5´ and 3´ endings, and the sequences were filtered based on their size and quality. The surviving merged pairs were de-replicated and the resulting unique sequences were clustered in operational taxonomic units OTUs. Singletons and chimeras were removed resulting in 33,220 and 13,323 for the 16S-rRNA-V4 and ITS2, respectively. The renamed merged pairs were mapped against the resulting OTUs to generate an OTU table. The OTUs were annotated using the sintax algorithm with a bootstrap threshold of 0.80 using the RDP database for 16S-rRNA-V4 and the Unite database for ITS2.

Low abundant OTUs were removed based on the thresholds previously determined[3]. OTUs present with a high read count in the negative controls, and OTUs that were classified as

non-microbial (e. g. plant, chloroplast, mitochondria) were removed. Samples with less than 1000 reads were removed. Finally, we obtained 236 samples with 1,164 OTUS for the 16S-rRNA-V4 amplicon and 199 samples with 1,416 OTUs for the ITS2 amplicon. Finally, the 16S-rRNA and the ITS2 of the inoculated strains were mapped to the generated OTUs using VSEARCH(--usearch_global) at 97 and 95% of similarity, respectively (Table S6).

The generated raw reads have been deposited under the SRA accessions SRR18063421 to SRR18063568 (Bioproject PRJNA808160).

Statistical analyses

The phyllospheric microbial communities were analyzed in terms of alpha and beta diversity, OTU abundance, and network structure. All the data analyses and plots were made using R software (version 4.1.1)[40]. Plots were made using the package ggplot2[41] and pheatmap[42]. *In-house* R scripts and data used for each step have been deposited at github.com/vicflonun/AgaviSyncoms.

First, the OTU table was rarefied to the minimum read count (794 and 3022 for 16S-rRNA and ITS2, respectively) and the OTU richness and Shannon indexes were calculated. Beta diversity was estimated using the binary Bray-Curtis distance between samples, then the distance matrix was used to ordinate the samples using a non-metric multidimensional scaling and the distance to their centroid was calculated. PERMANOVA of binary Bray-Curtis distances was used to identify the factors that influence the microbial community structure. All diversity indexes (OTU and carbon profiling), distances, and ordinations were calculated with the package vegan[43] and MASS[44] and their differences between groups of samples (season, treatments, and block) were tested using a Kruskal-Wallis test with a post hoc Dunn test.

Correlation networks and the differences in the relative abundance of OTUs and taxa between groups of samples were calculated and analyzed as reported in (V. M. F.-N, Citlali Fonseca-García, Damaris Desgarennes and L. P. P.-M. *in press).*

To test the influence of syncom treatment on plant growth, the changes per month of height, diameter, and unfolded leaves were calculated between February 2020 and November 2020 (n=6), and November 2020 and June 2021 (n=30). A t-test was performed to determine if the growth rate of treated plants, the number of rhizomatic suckers, and the amount of ^{o}Brix were significantly different from non-inoculated plants.

Metabolic profiling of the phyllospheric communities

The metabolic profiling of the phyllospheric microbial communities was performed using Eco-Biolog plates. This assay tests the ability of a microbial community to consume an array of 31 carbon sources. Two leaves per individual from each square in June 2021 (t19) were sampled and the phyllospheric microorganisms were obtained as explained before. The microbial pellet was resuspended in 5 ml of sterile phosphate buffer and the OD was adjusted to 0.5. The microbial suspension was inoculated in the plates using 100 µl per well. The plates were incubated in the darkness in a plastic box with wet paper towels to maintain humidity at 28°C for 4 days. The OD in the plates was recorded using a plate reader at 590 nm with a circular agitation of 20 seconds.

Leaf metabolomics

Metabolite extraction

Leaves of *A. tequila* plants were collected and disinfected at t12. Cuttings from the base of two leaves were taken (3 cm approx.) and freeze-dried. The lyophilized samples were ground in a mixer mill (Retsch MM400) for 35 seg at 30 m/seg. Five mg of lyophilized tissue were extracted with 500 µL of a mixture of methanol:acetonitrile:ethyl acetate at a 1:1:1 ratio under sonication for 30 min at room temperature. Samples were then centrifuged at 14,000 rpm for 10 min at 4 ^{o}C. The supernatant was recovered, transferred to a 1.5 mL Eppendorf tube, and the tube placed into a SpeedVac system to evaporate the solvent at room temperature. The dried extracts were weighed, resuspended at a concentration of 300 ng/µL (solution of water:acetonitrile at a 80:20 ratio), centrifuged at 14,000 rpm for 10 min at 4^{o}C, and the particle-free supernatant was recovered for further analysis. Equal volumes of all particle-free supernatants were mixed in one tube to prepare quality control (QC) samples.

Untargeted LC-MS^2 data acquisition

The metabolites were separated (2 µL sample injection) using an Agilent nanoLC 1260 Infinity system (Agilent Technologies, Inc., Santa Clara, CA) and a column packed with ZORBAX 80 SB-C18 (75 µm x 43 mm, 5 µm C18 with a 40 nL enrichment or trap column). Water and acetonitrile with 0.1% formic acid were used as mobile phases A and B at a flow rate of 300 nL/min and 2 µL for the nano (to separation column) and micro pumps (to enrichment column), respectively. The gradient started at 5% B, increased linearly to 20% B in 20 min, maintained at 20% B for 5 min, increased linearly to 100%, maintained at 100% B for 5 min, returned to 5% B in 1 min and then maintained at 5% B for 9 min before the next sample (to ensure column re-equilibration). Two blank samples (3 µL of mobile phases A and B at a 95:5 ratio) were run between experimental sample injections to minimize potential

carryover. The eluate from the column was delivered to a 6530 Accurate-Mass Q-TOF mass spectrometer (Agilent Technologies, Inc., Santa Clara, CA) via a HPLC-Chip Cube MS interface. Nanospray ionization under positive mode was employed. MS data was acquired using the following conditions: capillary voltage, 1850 V; gas temperature, 350 0C; drying gas flow, 5 L/min; skimmer voltage, 65 V; octapole RF, 750 V; fragmentor voltage, 175 V; spectra acquisition rate, 4 spectra/s over a mass range of 110 to 2000 m/z. MS^2 data conditions were: isolation window, narrow (1.3 m/z); spectra acquisition rate, 3 spectra/s; max precursors per cycle, 5 over a mass range of 50-2000 m/z. The active exclusion option was enabled, set to 2 spectra and release after 0.25 min. The ramped collision energy (CE) option was used with slope and offset values of 6 and 4, respectively. The instrument was externally calibrated before sample acquisition using ESI-L low mix concentration tuning mix solution (Agilent Technologies, Inc., Santa Clara, CA) to ensure a mass accuracy of <5 ppm for both MS and MS^2 data. Instrument performance was monitored during data acquisition by including QC samples every 3 experimental samples and evaluating the blank samples signals. Samples were randomly allocated for data acquisition.

LC-MS^2 data processing and analysis

We analyzed the LC-MS^2 datasets using a workflow comprised of open-access software packages and online platforms and following three main steps: 1) features were extracted and aligned among datasets using MZmine version 2.53[45]; 2) univariate and multivariate statistical analyses and hierarchical clustering visualization was done using Metaboanalyst 4.0 (https://www.metaboanalyst.ca)[46]; 3) automatic metabolite annotation or identification at the structure level[47] was performed using the Global Natural Products Social Molecular Networking web platform (GNPS, https://gnps.ucsd.edu) (Metabolomics Standards Initiative [MSI] classification level 2)[48] and *in-silico* tools (MolDiscovery, CSI:FingerID) (MSI, level 3)[49,50]. The chemical classes of the modulated metabolites (FC >1.5/1 or <1/1.5, *p-value* <0.05) (MSI, level 3) were retrieved by the CANOPUS tool[51,52] integrated within SIRIUS software version 4.9.12. The detailed processing parameters for all the pipelines are found in supplemental experimental methods in supporting information.

Data availability

The raw datasets have been deposited on the GNPS/MassIVE public repository[53] under the accession number MSV000089335. The parameters for classical molecular networking and spectral matching using all datasets are available on the following link: https://gnps.ucsd.edu/ProteoSAFe/status.jsp?task=fef5e3d881d049dd9a05cfa05ad8ac8e.

The MolDiscovery results are available on the following link: https://gnps.ucsd.edu/ProteoSAFe/status.jsp?task=186cab767a064f5b871914c6f7545aec.

Metabolomics statistical analysis

For the metabolomics data, features with reproducible quantification (based on QC coefficient of variation <30%) and fold change ≥ 1.5 or ≤ 1/1.5 and a p-value <0.05 (t-test) were considered as differentially abundant when comparing two groups. The abundance of selected metabolites was plotted as Box Plots depicting median and 10-90 percentile. For multivariate statistical analysis and heatmap visualization, Metaboanalyst 4.0 (https://www.metaboanalyst.ca) was utilized. Principal component analysis (PCA) was used to assess for sample clustering behavior and inter-group variation. Data was Log transformed (without scaling) for PCA and heatmap analysis.

Acknowledgments

We thank Devin Coleman-Derr and Robert Winkler for their constructive and helpful comments on an early version of our manuscript. We are also grateful to Javier and Eduardo Arroyo Solís, owners of the fields of *A. tequilana* plants used for this research and whose long-term collaboration has been key for developing our research. We thank J. Valeria Mendoza-Servín, Lizeth Dorantes Gómez, Gonzalo Córdova-López, and Eduardo Seynos-García, all members of the Microbial Interactions Lab, that helped with part of the field work. We also thank the support of Astri Lisset Rodríguez Miranda, Fernando Saúl Soto Camacho, Rosario Cornejo Lopez, and Yenetzi Villagrana Pacheco that helped in the laboratory work during their internships. LPPM acknowledges the financial support provided by CONACyT with grants A1-S-9889, FOINS-2015-01-0006, INFR-2012-01-187799 and CB-2010-01-151007.

Author contributions

VMFN and LPPM planned and designed research; VMFN designed syncoms and conducted most research and analyses; JACP, JDChG, RAV, MNVS helped perform experiments and the sampling of plants and microbial communities; AGHM, JXT, AMU analyzed plant metabolic data; VMFN and LPPM wrote paper; all authors revised and approved the final manuscript; and LPPM secured funding.

MAIN FIGURES

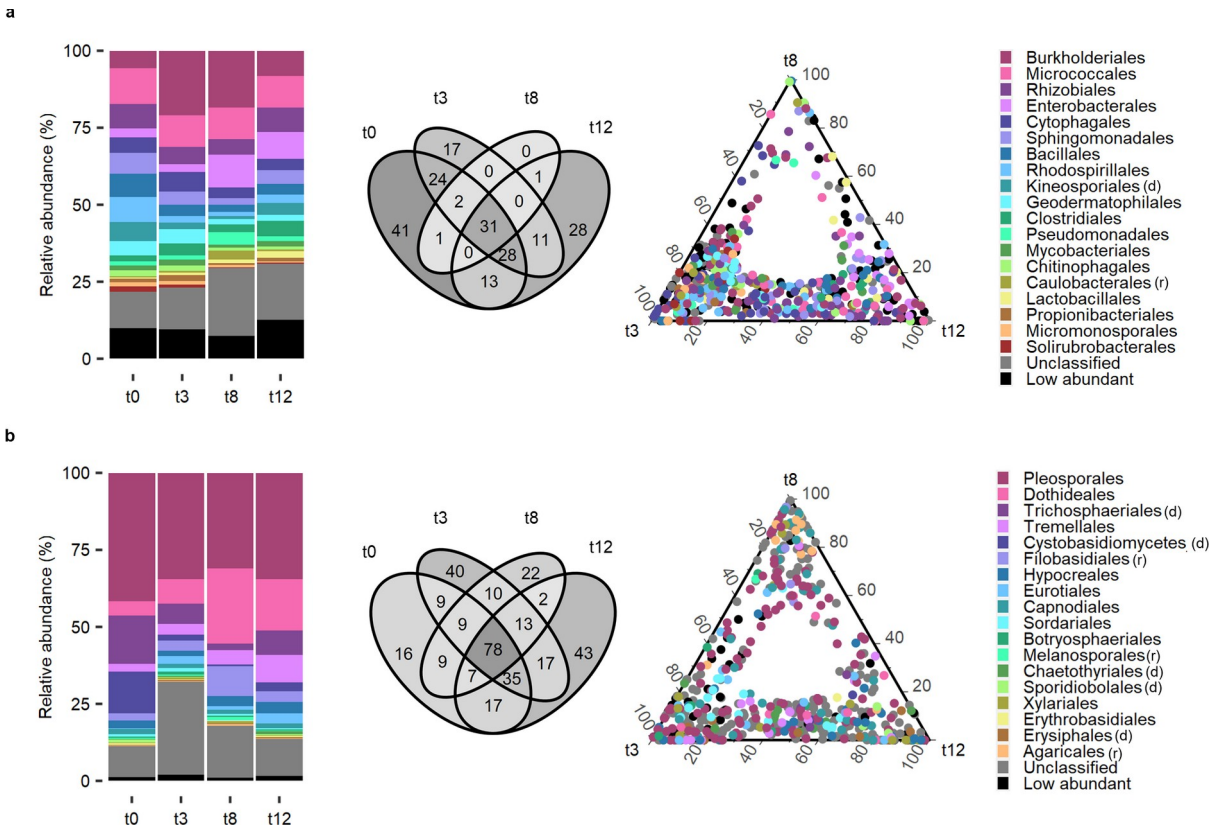

Fig. 1. Taxonomic classification, core, and enrichment analysis of prokaryotic (a) and eukaryotic (b) phyllospheric communities across sampling seasons. Bars represent the order-level relative abundance of OTUs. Venn diagrams show the number of shared OTUs (50% prevalence). Ternary plots show the ratio of the mean relative abundance of differential OTUs (Kruskal-Wallis test/Dunn test: FC >= |1.5| and adjusted p-value ≤ 0.05). Order-level enrichments are indicated with letters. d: enriched in dry season. r: enriched in rainy season (Wilcox test: FC >= |1.5| and adjusted p-value ≤ 0.05). Sampling seasons. t0:November 2019. t3:February 2020. t8:July 2020. t12:November 2020.

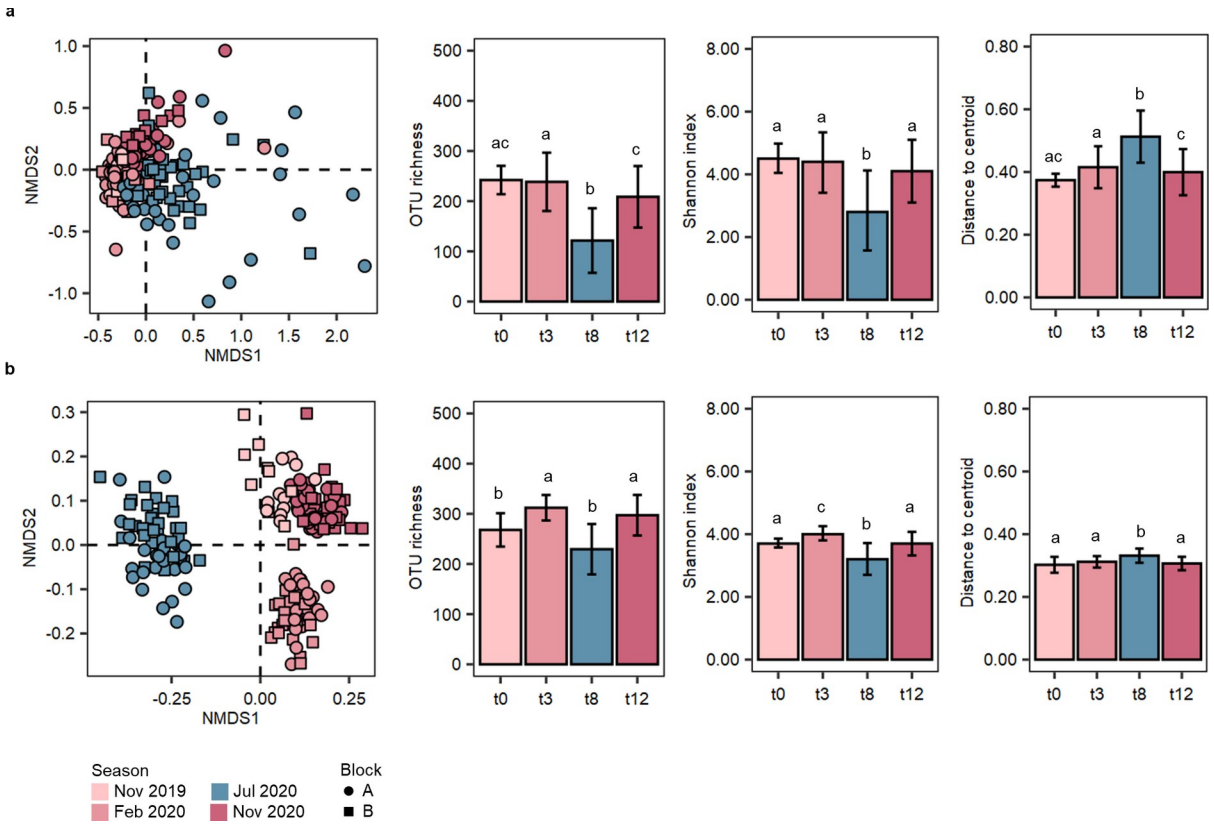

621 **Fig. 2. Diversity of the prokaryotic (a) and eukaryotic (b) phyllospheric communities**
622 **across sampling season.** Non-metric multidimensional scaling (NMDS) was calculated
623 using binary Bray-Curtis dissimilarities between samples. Bars represent the mean ± sd of
624 the observed OTU richness, Shannon index, and distance to the centroid of the
625 dissimilarities. Letters indicate significant changes between sampling seasons (Kruskal-
626 Wallis test/Dunn test: adjusted p-value ≤ 0.05). Sampling seasons: t0:November 2019.
627 t3:February 2020. t8:July 2020. t12:November 2020.
628

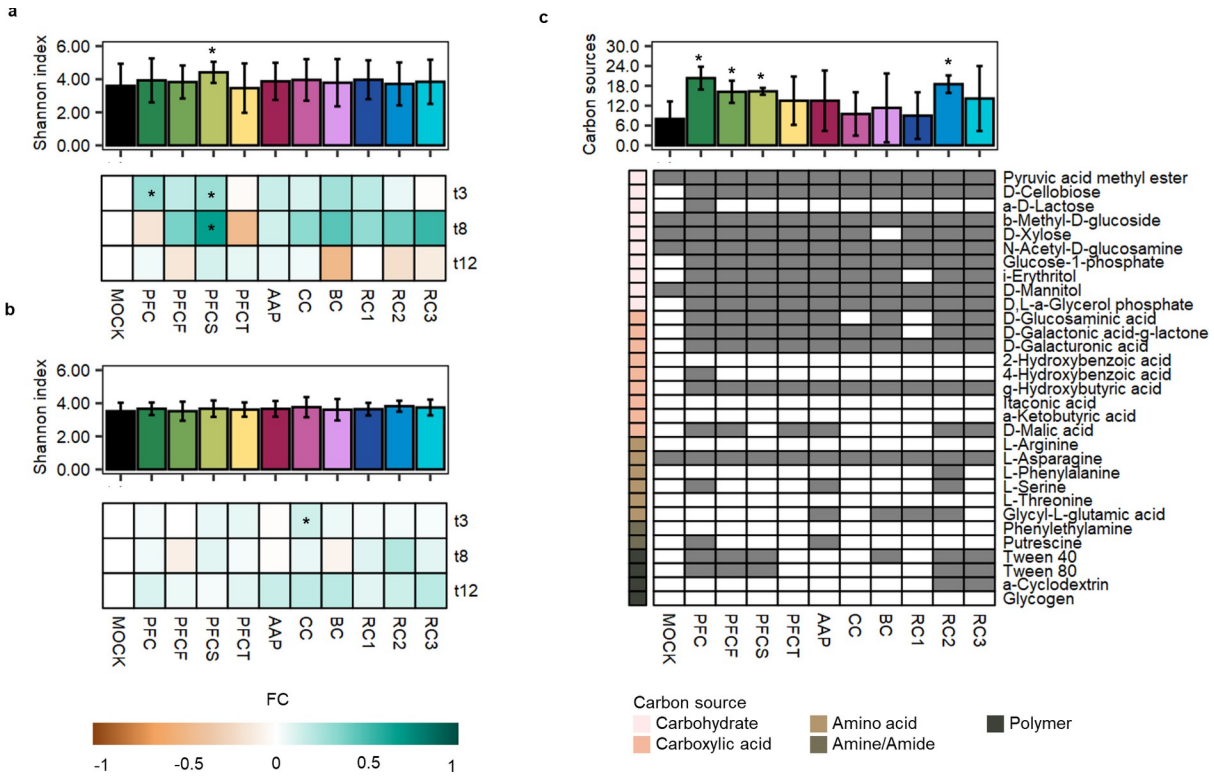

630 **Fig. 3. Taxonomic diversity (a,b) and carbon consumption profile (c) of phyllospheric**
631 **communities by syncom treatment.** Bars represent the mean ± sd of the Shannon index
632 of prokaryotic (a) and eukaryotic (b) phyllospheric communities by syncom treatment and the
633 heatmaps below show the fold change of the Shannon index between the syncom
634 treatments and the control (MOCK) in each sampling season (t3, t8, t12). The carbon
635 consumption profile (c) is represented as the mean ± sd of the number of carbon sources
636 consumed by the phyllospheric communities in June 2021 (t19) and the heatmap below
637 represents the unique carbon sources consumed by more than 50% of the samples in each
638 treatment. In all cases, an asterisk indicates a significant change between treatment and
639 control (Wilcox-test: p-value ≤ 0.05). Sampling seasons: t3:February 2020. t8:July 2020.
640 t12:November 2020.
641

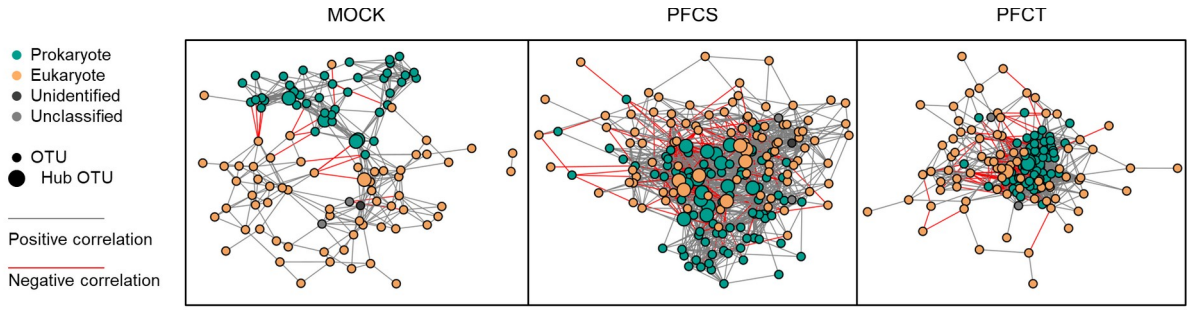

	MOCK	PFCS	PFCT
Nodes	51.20 ± 5.56	91.72 ± 6.73 (*)	69.70 ± 6.04 (*)
Edges	99.19 ± 19.92	398.39 ± 63.29 (*)	467.03 ± 85.66 (*)
Edges prokaryote – prokaryote (%)	51.60 ± 9.62	45.91 ± 6.88 (*)	52.94 ± 7.11
Edges prokaryote – eukaryote (%)	8.24 ± 3.44	25.93 ± 3.36 (*)	31.14 ± 3.97 (*)
Edges eukaryote – eukaryote (%)	40.16 ± 9.30	28.16 ± 6.07 (*)	15.93 ± 4.23 (*)
Number hubs	5.02 ± 1.79	12.86 ± 2.29 (*)	5.47 ±1.79
	POTU_43 g:*Methylobacterium*	POTU_18 g:*Sphingomonas* POTU_43 g:*Methylobacterium* POTU_89 g:*Sphingomonas* POTU_113 g:*Methylobacterium* POTU_164 g:*Sphingomonas* POTU_167 f:Sphingomonadaceae POTU_271 g:*Nocardioides*	POTU_14 g:*Bacillus* POTU_481 g:*Massilia*

643 **Fig. 4. Network analysis of the phyllospheric microbial communities by PFCS and**
644 **PFCT syncom treatment.** Correlation networks of the prokaryotic and fungal OTU counts
645 in the non-inoculated plants (MOCK) and plants inoculated with the PFCS and PFCT
646 syncoms. Vertices represent OTUs and edges represent significant correlation (Spearman
647 cor. ρ≥|0.6|) and p-value ≤0.01). Vertices are colored based on the OTU kingdom and edges
648 based on their weight. Red was used for negative correlations and black for positive
649 correlations. Bigger OTUs represent microbial hubs (above). Vertex and edge metrics (mean
650 ± sd) of 100 random correlation networks. Only hubs that matched the same genera or
651 OTU id of inoculated strains are shown (below). An asterisk indicates a significant change
652 between treatment and control (Wilcox-test: p-value ≤ 0.05)
653

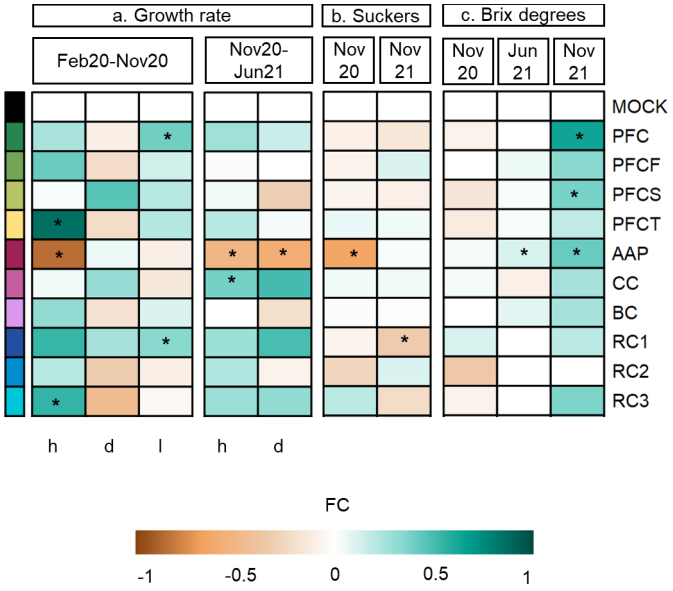

655 **Fig. 5. Growth and developmental changes in *A. tequilana* plants inoculated with**
656 **syncoms.** Heatmap represents the fold changes between the syncom treatments and the
657 control (MOCK) for the plant parameters measured. The changes in height (h), diameter (d),
658 and the number of leaves per month (l) were recorded from February 2020 (t3) to November
659 2020 (t12, n=6), while only height (h) and diameter (d) from November 2020 (t12) to June
660 2021 (t19, n=30, a). Rhizomatic suckers (b) were counted in November 2020 (t12) and 2021
661 (t24) while the °Brix (c) in the stem sap were measured in November 2020 (t12), June 2021
662 (t19), and November 2021 (t24). Asterix indicates a significant change between treatment
663 and control (Wilcox-test: p-value ≤ 0.05).
664

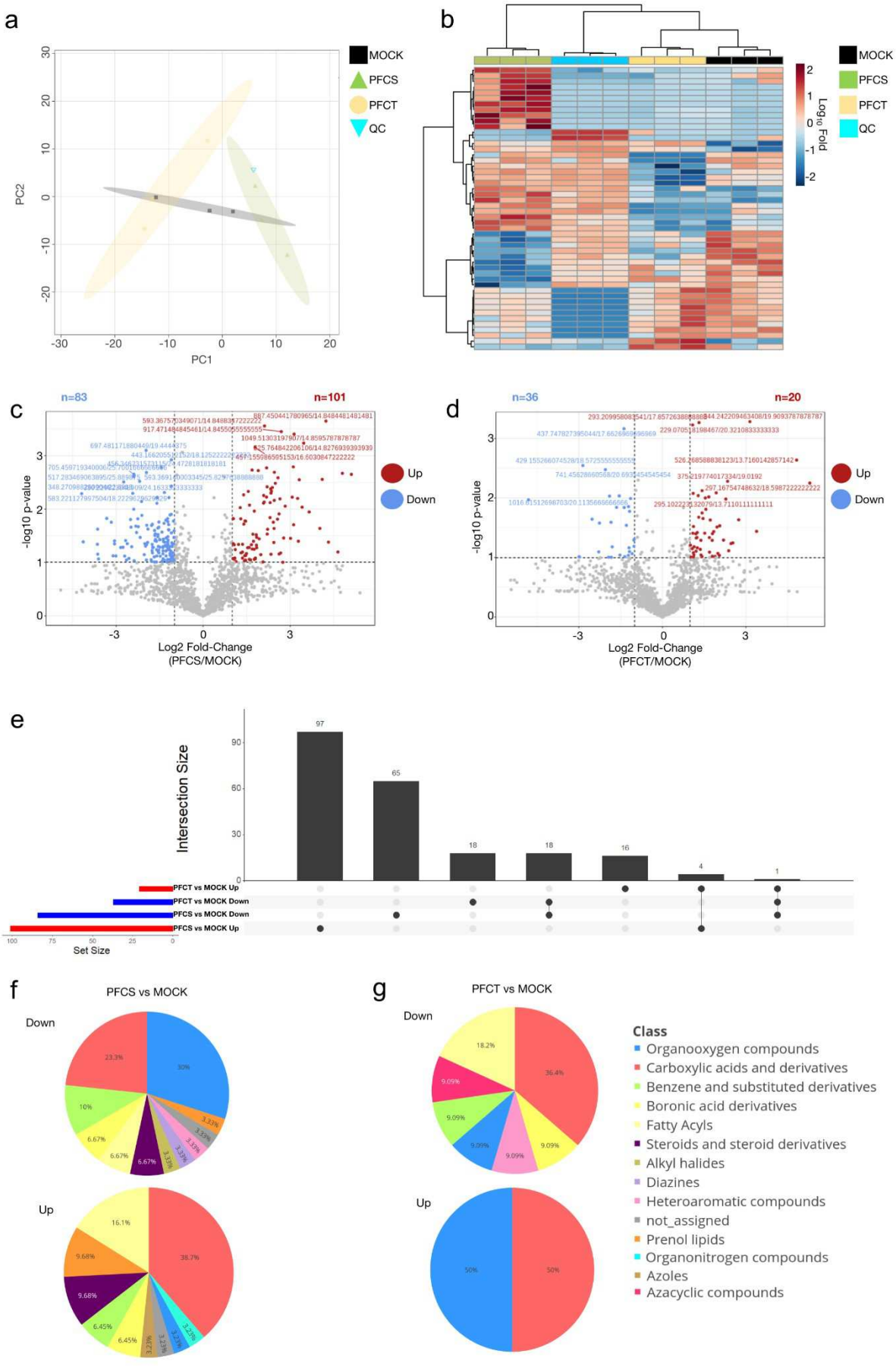
a
MOCK
PFCS
PFCT
QC
PC1
PC2
b
MOCK
PFCS
PFCT
QC
Log10 Fold
c
n=83
n=101
Up
Down
-log10 p-value
Log2 Fold-Change
(PFCS/MOCK)
d
n=36
n=20
Up
Down
-log10 p-value
Log2 Fold-Change
(PFCT/MOCK)
e
Intersection Size
97
65
18
18
16
4
1
PFCT vs MOCK Up
PFCT vs MOCK Down
PFCS vs MOCK Down
PFCS vs MOCK Up
Set Size
f
PFCS vs MOCK
Down
Up
g
PFCT vs MOCK
Down
Up
Class
Organooxygen compounds
Carboxylic acids and derivatives
Benzene and substituted derivatives
Boronic acid derivatives
Fatty Acyls
Steroids and steroid derivatives
Alkyl halides
Diazines
Heteroaromatic compounds
not_assigned
Prenol lipids
Organonitrogen compounds
Azoles
Azacyclic compounds

Fig. 6. Mass spectrometry-based untargeted metabolomic and chemoinformatic analyses of *A. tequilana* plants inoculated with PFCS and PFCT syncoms. (a) Principal Component Analysis (PCA) and (b) heatmap visualization (of the top 50 metabolites ranked by ANOVA test) of the aligned features among treatments with reproducible quantification. Data was Log-transformed, but not scaled. Shade areas depict the 95% confidence intervals. Quantified features among (c) PFCS and MOCK and (d) PFCT and MOCK treatments. Differential abundant features were determined when reaching a fold change ≥ 1.5 or ≤ 1/1.5 and p-value <0.05 (t-test). (e) Overlapping pattern among treatments using the features modulated (based on fold change and t-test criteria) by syncoms. Chemical class (retrieved by CANOPUS tool) profile assigned to the down- and up-modulated features by (f) PFCS and (g) PFCT syncoms.

REFERENCES

1. Gentry, H. S. *Agaves of Continental North America*. (University of Arizona Press, 2004).
2. Nobel, P. S. *Cacti: biology and uses*. (Univ of California Press, 2002).
3. Coleman-Derr, D. *et al.* Plant compartment and biogeography affect microbiome composition in cultivated and native Agave species. *New Phytologist* **209**, 798–811 (2016).
4. Camarena-Pozos, D. A., Flores-Núñez, V. M., López, M. G., López-Bucio, J. & Partida-Martínez, L. P. Smells from the desert: M icrobial volatiles that affect plant growth and development of native and non-native plant species. *Plant, cell & environment* **42**, 1368–1380 (2019).
5. Camarena-Pozos, D., Flores-Núñez, V., López, M. & Partida-Martínez, L. Fungal volatiles emitted by members of the microbiome of desert plants are diverse and capable of promoting plant growth. *Environmental Microbiology* (2021).
6. Flores-Núñez, V. M. *et al.* Functional Signatures of the Epiphytic Prokaryotic Microbiome of Agaves and Cacti. *Front. Microbiol.* **10**, 3044 (2020).
7. Agler, M. T. *et al.* Microbial hub taxa link host and abiotic factors to plant microbiome variation. *PLoS biology* **14**, e1002352 (2016).
8. Moreno-Ulloa, A. *et al.* Chemical profiling provides insights into the metabolic machinery of hydrocarbon-degrading deep-sea microbes. *Msystems* **5**, e00824-20 (2020).
9. Karray, F. *et al.* Climatic Aridity Gradient Modulates the Diversity of the Rhizosphere and Endosphere Bacterial Microbiomes of Opuntia ficus-indica. *Frontiers in microbiology* **11**, 1622 (2020).
10. Gargouri, M. *et al.* Increasing aridity shapes beta diversity and the network dynamics of the belowground fungal microbiome associated with Opuntia ficus-indica. *Science of The Total Environment* **773**, 145008 (2021).

11. Katsoula, A., Vasileiadis, S., Karamanoli, K., Vokou, D. & Karpouzas, D. G. Factors Structuring the Epiphytic Archaeal and Fungal Communities in a Semi-arid Mediterranean Ecosystem. *Microb Ecol* **82**, 638–651 (2021).
12. Toju, H. *et al.* Core microbiomes for sustainable agroecosystems. *Nature Plants* **4**, 247–257 (2018).
13. van der Heijden, M. G. A. & Hartmann, M. Networking in the Plant Microbiome. *PLoS Biol* **14**, e1002378 (2016).
14. Pellegrini, M., Spera, D. M., Ercole, C. & Del Gallo, M. Allium cepa L. Inoculation with a Consortium of Plant Growth-Promoting Bacteria: Effects on Plants, Soil, and the Autochthonous Microbial Community. *Microorganisms* **9**, 639 (2021).
15. Shang, J. & Liu, B. Application of a microbial consortium improves the growth of *Camellia sinensis* and influences the indigenous rhizosphere bacterial communities. *J Appl Microbiol* **130**, 2029–2040 (2021).
16. Dos-Santos, C. M., Ribeiro, N. V. S., Schwab, S., Baldani, J. I. & Vidal, M. S. The Effect of Inoculation of a Diazotrophic Bacterial Consortium on the Indigenous Bacterial Community Structure of Sugarcane Apoplast Fluid. *Curr Microbiol* **78**, 3079–3091 (2021).
17. Ratzke, C., Barrere, J. & Gore, J. Strength of species interactions determines biodiversity and stability in microbial communities. *Nat Ecol Evol* **4**, 376–383 (2020).
18. Liu, H. *et al.* Effective colonisation by a bacterial synthetic community promotes plant growth and alters soil microbial community. *J of Sust Agri & Env* **1**, 30–42 (2022).
19. Qin, C. *et al.* Responses of phyllosphere microbiota and plant health to application of two different biocontrol agents. *AMB Expr* **9**, 42 (2019).
20. Carlström, C. I. *et al.* Synthetic microbiota reveal priority effects and keystone strains in the Arabidopsis phyllosphere. *Nature ecology & evolution* **3**, 1445–1454 (2019).
21. Banerjee, S., Schlaeppi, K. & van der Heijden, M. G. A. Keystone taxa as drivers of microbiome structure and functioning. *Nat Rev Microbiol* **16**, 567–576 (2018).

22. Berry, D. & Widder, S. Deciphering microbial interactions and detecting keystone species with co-occurrence networks. *Front. Microbiol.* **5**, (2014).
23. Tan, J., Kerstetter, J. E. & Turcotte, M. M. Eco-evolutionary interaction between microbiome presence and rapid biofilm evolution determines plant host fitness. *Nat Ecol Evol* **5**, 670–676 (2021).
24. Monier, J.-M. & Lindow, S. E. Aggregates of Resident Bacteria Facilitate Survival of Immigrant Bacteria on Leaf Surfaces. *Microb Ecol* **49**, 343–352 (2005).
25. Alsharif, W., Saad, M. M. & Hirt, H. Desert Microbes for Boosting Sustainable Agriculture in Extreme Environments. *Front. Microbiol.* **11**, 1666 (2020).
26. Finkel, O. M., Castrillo, G., Herrera Paredes, S., Salas González, I. & Dangl, J. L. Understanding and exploiting plant beneficial microbes. *Current Opinion in Plant Biology* **38**, 155–163 (2017).
27. Nobel, P. & Valenzuela, A. Environmental responses and productivity of the CAM plant, Agave tequilana. *Agricultural and Forest Meteorology* **39**, 319–334 (1987).
28. Abanda-Nkpwatt, D., Musch, M., Tschiersch, J., Boettner, M. & Schwab, W. Molecular interaction between Methylobacterium extorquens and seedlings: growth promotion, methanol consumption, and localization of the methanol emission site. *Journal of Experimental Botany* **57**, 4025–4032 (2006).
29. Green, P. N. & Ardley, J. K. Review of the genus Methylobacterium and closely related organisms: a proposal that some Methylobacterium species be reclassified into a new genus, Methylorubrum gen. nov. *International Journal of Systematic and Evolutionary Microbiology* **68**, 2727–2748 (2018).
30. Sidana, J., Singh, B. & Sharma, O. P. Saponins of Agave: Chemistry and bioactivity. *Phytochemistry* **130**, 22–46 (2016).
31. Almaraz-Abarca, N., Delgado-Alvarado, E. A., Antonio'Avila-Reyes, J., Uribe-Soto, J. N. & González-Valdez, L. S. The phenols of the genus Agave (Agavaceae). (2013).
32. Jin, Y.-L. *et al.* A new steroidal saponin, yuccalan, from the leaves ofYucca smalliana. *Arch Pharm Res* **30**, 543–546 (2007).

758 33. Desgarennes, D., Garrido, E., Torres-Gomez, M. J., Pena-Cabriales, J. J. & Partida-
759 Martinez, L. P. Diazotrophic potential among bacterial communities associated with wild
760 and cultivated Agave species. *FEMS microbiology ecology* **90**, 844–857 (2014).
761 34. Lundberg, D. S., Yourstone, S., Mieczkowski, P., Jones, C. D. & Dangl, J. L. Practical
762 innovations for high-throughput amplicon sequencing. *Nat Methods* **10**, 999–1002
763 (2013).
764 35. FastQC. (2015).
765 36. Weber, N. *et al.* Nephele: a cloud platform for simplified, standardized and reproducible
766 microbiome data analysis. *Bioinformatics* **34**, 1411–1413 (2018).
767 37. Bolger, A. M., Lohse, M. & Usadel, B. Trimmomatic: a flexible trimmer for Illumina
768 sequence data. *Bioinformatics* **30**, 2114–2120 (2014).
769 38. Magoc, T. & Salzberg, S. L. FLASH: fast length adjustment of short reads to improve
770 genome assemblies. *Bioinformatics* **27**, 2957–2963 (2011).
771 39. Rognes, T., Flouri, T., Nichols, B., Quince, C. & Mahé, F. VSEARCH: a versatile open
772 source tool for metagenomics. *PeerJ* **4**, e2584 (2016).
773 40. R Core Team. *R: A Language and Environment for Statistical Computing*. (R Foundation
774 for Statistical Computing, 2021).
775 41. Wickham, H. *ggplot2: Elegant Graphics for Data Analysis*. (Springer-Verlag New York,
776 2016).
777 42. Kolde, R. & others. Pheatmap: pretty heatmaps. *R package version* **1**, 747 (2012).
778 43. Oksanen, J. Multivariate Analysis of Ecological Communities in R: vegan tutorial. 43
779 (2019).
780 44. Venables, W. N. & Ripley, B. D. *Modern Applied Statistics with S*. (Springer, 2002).
781 45. Pluskal, T., Castillo, S., Villar-Briones, A. & Orešič, M. MZmine 2: modular framework for
782 processing, visualizing, and analyzing mass spectrometry-based molecular profile data.
783 *BMC bioinformatics* **11**, 1–11 (2010).
784 46. Chong, J. *et al.* MetaboAnalyst 4.0: towards more transparent and integrative
785 metabolomics analysis. *Nucleic acids research* **46**, W486–W494 (2018).

786 47. Schymanski, E. L. *et al.* Identifying small molecules via high resolution mass
787 spectrometry: communicating confidence. (2014).
788 48. Aron, A. T. *et al.* Reproducible molecular networking of untargeted mass spectrometry
789 data using GNPS. *Nature protocols* **15**, 1954–1991 (2020).
790 49. Dührkop, K., Shen, H., Meusel, M., Rousu, J. & Böcker, S. Searching molecular
791 structure databases with tandem mass spectra using CSI: FingerID. *Proceedings of the*
792 *National Academy of Sciences* **112**, 12580–12585 (2015).
793 50. Cao, L. *et al.* MolDiscovery: learning mass spectrometry fragmentation of small
794 molecules. *Nat Commun* **12**, 3718 (2021).
795 51. Dührkop, K. *et al.* Systematic classification of unknown metabolites using high-resolution
796 fragmentation mass spectra. *Nature Biotechnology* **39**, 462–471 (2021).
797 52. Djoumbou Feunang, Y. *et al.* ClassyFire: automated chemical classification with a
798 comprehensive, computable taxonomy. *Journal of cheminformatics* **8**, 1–20 (2016).
799 53. Wang, M. *et al.* Sharing and community curation of mass spectrometry data with Global
800 Natural Products Social Molecular Networking. *Nature biotechnology* **34**, 828–837
801 (2016).

802

Supplementary Files

This is a list of supplementary files associated with this preprint. Click to download.

- SupplementaryInformationSyncomsAtequilanaVMFNLPPM220621.pdf